Ultrafast Dynamics in Aqueous Polyacrylamide Solutions

Hideaki Shirota*,† and Edward W. Castner, Jr.*

Contribution from the Department of Chemistry and Chemical Biology, Rutgers, The State University of New Jersey, 610 Taylor Road, Piscataway, New Jersey 08854-8087

Received February 1, 2001

Abstract: We have investigated the ultrafast dynamics of aqueous polyacrylamide ($[-CH_2CH(CONH_2)-]_n$, or PAAm) solutions using femtosecond optical heterodyne-detected Raman-induced Kerr effect spectroscopy (OHD-RIKES). The observed aqueous PAAm dynamics are nearly identical for both $M_w = 1500$ and 10 000. Aqueous propionamide ($CH_3CH_2CONH_2$, or PrAm) solutions were also studied, because PrAm is an exact model for the PAAm constitutional repeat unit (CRU). The longest time scale dynamics observed for both aqueous PAAm and PrAm solutions occur in the 4−10 ps range. Over the range of concentrations from 0 to 40 wt %, the picosecond reorientation time constants for the aqueous PAAm and PrAm solutions scale linearly with the solution concentration, despite the fact that the solution shear viscosities vary exponentially from 1 to 264 cP. For a given value of solution concentration in weight percent, constant ratios of measured reorientation time constants for PAAm to PrAm are obtained. This ratio of PAAm to PrAm reorientation time constants is equal to the ratio of the volume for the PAAm constitutional repeat unit ($-CH_2CHCONH_2-$) to the molecular volume of PrAm. For these reasons, we assign the polymer reorientation dynamics to motions of the entire constitutional repeat unit, not only side group motions. Simple molecular dynamics simulations of $H[-CH_2-CH(CONH_2)-]_7H$ in a periodic box with 180 water molecules support this assignment. Amide−amide and amide−water hydrogen-bonding interactions lead to strongly oscillatory femtosecond dynamics in the Kerr transients, peaking at 80, 410, and 750 fs.

Introduction

Polyacrylamide ($[-CH_2CH(CONH_2)-]_n$, or PAAm) belongs to a unique class of water-soluble polymers. PAAm is the first polymer for which the volume phase transition in the polymer gel was observed.[1] PAAm is most widely known within the research community for its use as a cross-linked hydrogel for size-based electrophoretic separation of proteins and nucleic acids—these methods are known as polyacrylamide gel electrophoresis (PAGE) (and SDS−PAGE when used in combination with the surfactant sodium dodecyl sulfate). The primary industrial use for PAAm is in the linear form, where it is used as a soil additive to prevent erosion.

PAAm has a hydrophobic main chain and a hydrophilic side group. As can be seen in the model shown in Figure 1a, one may consider PAAm to be a polyethylene main chain with formamido side groups. Aqueous PAAm solutions are very inhomogeneous at the molecular level, as shown by both experiments[2−5] and simulations.[6−12] We present here the first optical spectroscopy investigations of the ultrafast dynamics in aqueous PAAm solutions. Our data permit exploration of the connection between local frictional forces, hydrogen bond interactions, and the macroscopic shear viscosity of aqueous PAAm solutions.

Both the static and dynamic features of polymer solutions depend strongly on polymer−polymer and polymer−solvent interactions, polymerization degree (molecular weight), concentration, and temperature.[13−16] Aqueous macromolecular systems are even more complex because both inter- and intramolecular hydrogen bonds are present.[17−22] Hydrogen bonds occurring between polymer−water and polymer−polymer often determine the function of the system. Water molecules in aqueous macromolecular solutions can usually be classified into one of three categories: (i) strongly interacting or nonfreezing water, (ii) bound or intermediate water, and (iii) free or bulklike water.[23] The ultrafast dynamics of interfacial water is an active

* Address correspondence to either author. E-mail: cshirota@mail.ecc.u-tokyo.ac.jp, castner@rutchem.rutgers.edu.

† Present address: Department of General Systems Sciences, Graduate School of Arts and Sciences, University of Tokyo, 3-8-1 Komaba, Meguro-ku, Tokyo153-8902, Japan.

(1) Tanaka, T. *Phys. Rev. Lett.* **1978**, *40*, 820.
(2) Maeda, Y.; Tsukida, N.; Kitano, H.; Terada, T.; Yamanaka, J. *J. Phys. Chem.* **1993**, *97*, 13903.
(3) Terada, T.; Maeda, Y.; Kitano, H. *J. Phys. Chem.* **1993**, *97*, 3619.
(4) Tsukida, N.; Muranaka, H.; Ide, M.; Maeda, Y.; Kitano, H. *J. Phys. Chem. B* **1997**, *101*, 6676.
(5) Kitano, H.; Sudo, K.; Ichikawa, K.; Ide, M.; Ishihara, K. *J. Phys. Chem. B* **2000**, *104*, 11425.
(6) Tamai, Y.; Tanaka, H.; Nakanishi, K. *Mol. Simul.* **1996**, *16*, 359.
(7) Tamai, Y.; Tanaka, H.; Nakanishi, K. *Macromolecules* **1996**, *29*, 6750.
(8) Tamai, Y.; Tanaka, H.; Nakanishi, K. *Macromolecules* **1996**, *29*, 6761.
(9) Muller-Plathe, F.; van Gunsteren, W. F. *Polymer* **1997**, *38*, 2259.
(10) Muller-Plathe, F. *J. Chem. Phys.* **1998**, *108*, 8252.
(11) Muller-Plathe, F. *Macromolecules* **1998**, *31*, 6721.
(12) Netz, P. A.; Dorfmuller, T. *J. Phys. Chem. B* **1998**, *102*, 4875.
(13) Flory, P. J. *Principles of Polymer Chemistry*; Cornell University Press: Ithaca, NY, 1953.
(14) de Gennes, P. D. *Scaling Concepts in Polymer Physics*; Cornell University Press: Ithaca, NY, 1979.
(15) Doi, M.; Edwards, S. F. *The Theory of Polymer Dynamics*; Oxford University Press: Oxford, 1986.
(16) Strobl, G. R. *The Physics of Polymers*, 2nd ed.; Springer: Berlin, 1997.
(17) Kuntz, I. D. J.; Kauzmann, W. *Adv. Protein Chem.* **1974**, *28*, 239.
(18) Sänger, W. *Annu. Rev. Biophys. Biophys. Chem.* **1987**, *16*, 93.
(19) Teeter, M. M. *Annu. Rev. Biophys. Biophys. Chem.* **1991**, *20*, 577.
(20) Pethig, R. *Annu. Rev. Phys. Chem.* **1992**, *43*, 177.
(21) Otting, G.; Liepinsh, E. *Acc. Chem. Res.* **1995**, *28*, 171.
(22) Nandi, N.; Bhattacharyya, K.; Bagchi, B. *Chem. Rev.* **2000**, *100*, 2013.

10.1021/ja010290z CCC: $20.00
Published on Web 12/01/2001

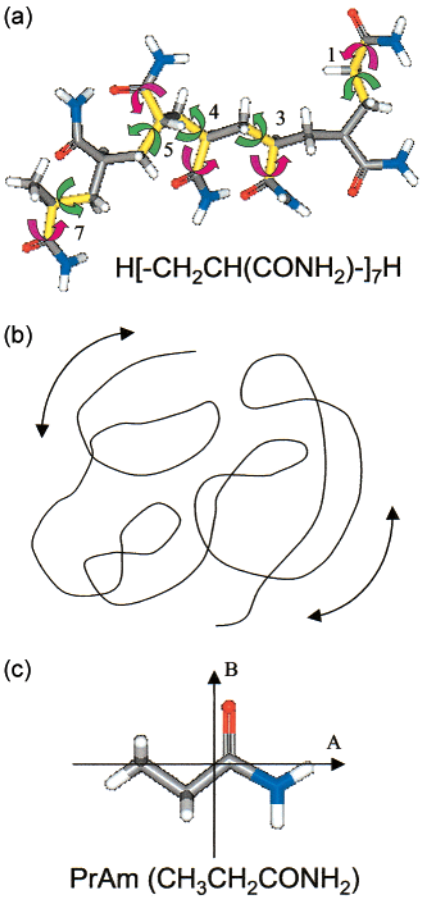

Figure 1. (a) Local motions of the PAAm heptamer. Bonds for which torsion angles are analyzed are highlighted in yellow. Side group torsions are indicated by the magenta arrows, main chain torsions by the green arrows. (b) Pictorial model for the orientational motion of an entire polymer chain in solution. (c) PrAm and its inertial rotation axes A and B.

field of research: Nandi et al. have recently reviewed work on several classes of systems, including proteins, DNA, normal and reverse micelles, liposomes, cyclodextrins, polymers, metal oxide nanoparticles, and others.[22]

The study of liquid water dynamics has a rich history.[24,25] Recently, investigations of water using ever more sophisticated spectroscopic techniques have resulted in continually better data quality. The works of both Schmuttenmaer and co-workers and Keiding and co-workers have probed liquid water dynamics using THz spectroscopy.[26−30] In addition to superior signal-to-noise ratios, a significant advantage of THz experiments is that both the dielectric absorption and dispersion spectra can be obtained simultaneously. Using femtosecond Raman methods, several groups have previously reported biexponential relaxation for the diffusive reorientation dynamics of liquid water, consistent with the THz relaxation data.[31−34] Recently, Vöhringer and co-workers have used a rapid-scan technique to average thousands of scans to obtain even better quality signals. Their analysis shows that a triexponential function may be the best description for the diffusive reorientation in water at certain elevated temperatures, although room-temperature water is best fit to a biexponential function.[35] Analysis of the full intermolecular spectrum for water shows a combination of two (or more) exponential relaxations, two density fluctuation bands at about 50 and 180 cm^{-1}, and a very broad librational band peaked near 600 cm^{-1}, which neutron scattering and other methods have assigned to three distinct librations at 440, 540, and 770 cm^{-1}.[25]

Optical heterodyne-detected Raman-induced Kerr effect spectroscopy (OHD-RIKES) is a nonlinear optical polarization technique that measures the depolarized Raman signal from a transparent liquid in the time domain; the depolarized Raman spectrum is obtained by direct Fourier transform deconvolution. Using OHD-RIKES, the solution dynamics are obtained on time scales ranging from tens of femtoseconds to hundreds of picoseconds. This technique is frequently used to investigate the microscopic aspects of the ultrafast dynamics of neat liquids,[31−34,36−72] binary solutions,[40−42,48,52,70] supercooled liquids,[73,74] and confined solvent molecules.[75−80]

Here we report the ultrafast dynamics of three kinds of aqueous solutions: two chain lengths of PAAm, with weight-averaged molecular weights M_w of 1500 and 10 000, and PrAm.

(23) Jeffrey, G. A.; Saenger, W. *Hydrogen Bonding in Biological Structures*, 1st ed.; Springer-Verlag: Berlin, 1991.
(24) Franks, F. *The Physics and Physical Chemistry of Water*, 1st ed.; Plenum Press: New York and London, 1972; Vol. 1.
(25) Walrafen, G. E. In *Raman and Infrared Spectral Investigations of Water Structure*; Franks, F., Ed.; Plenum Press: New York, 1972; Vol. 1.
(26) Kindt, J. T.; Schmuttenmaer, C. A. *J. Phys. Chem.* **1996**, *100*, 10373.
(27) Kindt, J. T.; Schmuttenmaer, C. A. *J. Chem. Phys.* **1997**, *106*, 4389.
(28) Thrane, L.; Jacobsen, R. H.; Jepsen, P. U.; Keiding, S. R. *Chem. Phys. Lett.* **1995**, *240*, 330.
(29) Rønne, C.; Thrane, L.; Åstrand, P. O.; Wallqvist, A.; Mikkelsen, K. V.; Keiding, S. R. *J. Chem. Phys.* **1997**, *107*, 5319.
(30) Rønne, C.; Åstrand, P. O.; Keiding, S. R. *Phys. Rev. Lett.* **1999**, *82*, 2888.
(31) Chang, Y. J.; Castner, E. W., Jr. *J. Chem. Phys.* **1993**, *99*, 7289.
(32) Castner, E. W., Jr.; Chang, Y. J.; Chu, Y. C.; Walrafen, G. E. *J. Chem. Phys.* **1995**, *102*, 653.
(33) Palese, S.; Schilling, L.; Miller, R. J. D.; Staver, P. R.; Lotshaw, W. T. *J. Phys. Chem.* **1994**, *98*, 6308.
(34) Palese, S.; Mukamel, S.; Miller, R. J. D.; Lotshaw, W. T. *J. Phys. Chem.* **1996**, *100*, 10380.
(35) Winkler, K.; Lindner, J.; Bursing, H.; Vohringer, P. *J. Chem. Phys.* **2000**, *113*, 4674.
(36) McMorrow, D.; Lotshaw, W. T.; Kenney-Wallace, G. A. *IEEE J. Quantum Electron.* **1988**, *24*, 443.
(37) McMorrow, D.; Lotshaw, W. T. *Chem. Phys. Lett.* **1990**, *174*, 85.
(38) McMorrow, D.; Lotshaw, W. T. *J. Phys. Chem.* **1991**, *95*, 10395.
(39) McMorrow, D.; Lotshaw, W. T. *Chem. Phys. Lett.* **1991**, *178*, 69.
(40) Lotshaw, W. T.; McMorrow, D.; Thantu, N.; Melinger, J. S.; Kitchenham, R. *J. Raman Spectrosc.* **1995**, *26*, 571.
(41) McMorrow, D.; Thantu, N.; Melinger, J. S.; Kim, S. K.; Lotshaw, W. T. *J. Phys. Chem.* **1996**, *100*, 10389.
(42) Chang, Y. J.; Castner, E. W., Jr. *J. Chem. Phys.* **1993**, *99*, 113.
(43) Chang, Y. J.; Castner, E. W., Jr. *J. Phys. Chem.* **1994**, *98*, 9712.
(44) Chang, Y. J.; Castner, E. W., Jr. *J. Phys. Chem.* **1996**, *100*, 3330.
(45) Castner, E. W., Jr.; Chang, Y. J.; Melinger, J. S.; McMorrow, D. *J. Luminesc.* **1994**, *60−1*, 723.
(46) Castner, E. W., Jr.; Chang, Y. J. In *Ultrafast Phenomena X*; Barbara, P. F., Fujimoto, J., Knox, W. Zinth, W., Eds.; Springer-Verlag: Berlin, 1996; pp 296−297.
(47) Castner, E. W., Jr.; Maroncelli, M. *J. Mol. Liq.* **1998**, *77*, 1.
(48) Smith, N. A.; Lin, S.; Meech, S. R.; Shirota, H.; Yoshihara, K. *J. Phys. Chem. A* **1997**, *101*, 9578.
(49) Smith, N. A.; Lin, S.; Meech, S. R.; Yoshihara, K. *J. Phys. Chem. A* **1997**, *101*, 3641.
(50) Shirota, H.; Yoshihara, K.; Smith, N. A.; Lin, S.; Meech, S. R. *Chem. Phys. Lett.* **1997**, *281*, 27.
(51) Smith, N. A.; Meech, S. R. *Faraday Discuss.* **1997**, *108*, 35.
(52) Smith, N. A.; Meech, S. R. *J. Phys. Chem. A* **2000**, *104*, 4223.
(53) Quitevis, E. L.; Neelakandan, M. *J. Phys. Chem.* **1996**, *100*, 10005.
(54) Neelakandan, M.; Pant, D.; Quitevis, E. L. *Chem. Phys. Lett.* **1997**, *265*, 283.
(55) Neelakandan, M.; Pant, D.; Quitevis, E. L. *J. Phys. Chem. A* **1997**, *101*, 2936.
(56) Kamada, K.; Ueda, M.; Sakaguchi, T.; Ohta, K.; Fukumi, T. *Chem. Phys. Lett.* **1996**, *249*, 329.
(57) Kamada, K.; Ueda, M.; Ohta, K.; Wang, Y.; Ushida, K.; Tominaga, K. *J. Chem. Phys.* **1998**, *109*, 10948.
(58) Kamada, K.; Sugino, T.; Ueda, M.; Tawa, K.; Shimizu, Y.; Ohta, K. *Chem. Phys. Lett.* **1999**, *302*, 615.
(59) Kinoshita, S.; Kai, Y.; Yamaguchi, M.; Yagi, T. *Phys. Rev. Lett.* **1995**, *75*, 148.
(60) Kinoshita, S.; Kai, Y.; Yamaguchi, M.; Yagi, T. *Chem. Phys. Lett.* **1995**, *236*, 259.

Femtosecond OHD-RIKES transients were recorded for concentrations of 0, 5, 10, 20, 30, and 40 wt % PAAm and PrAm in water. As illustrated schematically in Figure 1b, the overall dynamics for polymer chains can be greatly influenced by self-chain or entanglement interactions. For chains exceeding a critical length, the viscosity increases sharply, scaling as the 3.4 power of the molecular weight.[13−16] Interchain entanglements increase greatly above a critical concentration.[81] Self-entanglement effects will not dominate the behavior of M_w = 1500 PAAm, which has only 21 constitutional repeat units, but will become more significant for the longer chains with M_w = 10 000. The critical concentration for self-entanglement, c^*, can be estimated on the basis of molecular weight or from the intrinsic viscosity at which deviations from which Θ-behavior occur.[81] Using the relation $c^* = M_w^{-0.6}$, we estimate that interchain entanglement occurs at quite low weight percent concentrations of polymer, so that our solutions of ≥10 wt % are all above the concentration for entanglement.

The nonlinear viscosity increase for longer polymer chains is one cause for the breakdown of simple hydrodynamic models when applied to polymer solutions. On a local scale, one may consider the polymer dynamics to be largely influenced by main chain or side group torsional motions. To aid in the assignment of the observed dynamics, we carried out simple molecular dynamics computer simulations for an aqueous PAAm chain with n = 7. The arrows in Figure 1a indicate some of the important torsional motions for a short polyacrylamide chain with n = 7. To better understand the local motions of and within a single constitutional repeat unit of PAAm, we have used aqueous PrAm (shown in Figure 1c) as a model. The diffusive behavior of aqueous PrAm solutions obeys hydrodynamic scaling laws, as expected.

Experimental Section

Sample Preparation. Aqueous polyacrylamide solutions (Aldrich, 50 wt %, M_w = 1500 and 10 000) were used as received. Solid propionamide was also used as received from Aldrich. Water was obtained from a Millipore Milli-Q purification system (distilled, deionized, with conductivity of 18.2 MΩ cm). To reduce light scatter, the sample solutions were filtered through a 0.45-μm PTFE filter (Millipore).

Viscosity Measurements. The viscosities of aqueous PAAm and PrAm solutions were measured with Cannon-Fenske viscometers (International Research Glassware; size number 50, 100, and 150) at 293 ± 0.1 K. The temperature was regulated with a Neslab RTE-111 refrigerated bath/circulator. The measured kinematic viscosity, $\eta_{kinematic}$, is converted to the absolute viscosity η by $\eta = \rho\eta_{kinematic}$, where the ρ is the measured density of the sample solution.

Femtosecond OHD-RIKES Measurements. The OHD-RIKES instrument is based on published designs[36,38,42] and uses a laboratory-built femtosecond Ti:sapphire laser operating at 795 nm center wavelength.[82] The laser pulse cross-correlation measured with a 50 μm KDP crystal was 44 ± 3 fs fwhm (equivalent to a 28 ± 2 fs pulse, assuming a sech^2 pulse shape). The measured spectral bandwidth of the laser was 40 nm. All the measurements were made at 294 ± 1 K. Scans with high time resolution of 1024 points at 0.5 μm/step were recorded for a time window of 3.4 ps. The slower reorientational dynamics were captured in 36 ps scans with 15 μm per data point. For neat water, 15 scans with 2048 points at 0.5 μm/step were averaged. For the aqueous PAAm and PrAm solutions, 15 scans were averaged for the short time window transients, and 30 scans were averaged for the longer ones.

Fourier transform deconvolution of the OHD-RIKES data is carried out as described previously.[37,38] Under the polarization conditions used, the resulting frequency domain spectrum is equivalent to the low-frequency depolarized Raman spectrum multiplied by the Bose−Einstein thermal occupation factor.[31] Precise details of both the OHD-RIKES instrument and the Fourier transform deconvolution analysis of the OHD-RIKES transients are given in the Supporting Information.

The low-frequency spectra in liquids and solutions arise from both translational and reorientational dynamics. It is common to fit low-frequency spectra for liquids and solutions to a variety of line shapes, including multimode Brownian oscillators,[34,83,84] Ohmic,[50,67,85] and sums of antisymmetrized Gaussian line shapes.[31,32,43,44,48,49,52] We find that we obtain indistinguishable fits using line shape models that are sums of different combinations of Ohmic and antisymmetrized Gaussian line shapes. Figure 6 shows that equally good quality fits to our aqueous PAAm OHD-RIKES spectra are obtained with different line shape models—sums of two each Ohmic and antisymmetrized Gaussian functions, and sums of one Ohmic plus three antisymmetrized Gaussians. It is likely that given sufficient numbers of line shape parameters (in this case a sum of 4 line shapes with 12 adjustable parameters), intermolecular spectra can be fit to a variety of asymmetric line shapes, including Ohmic, antisymmetrized Gaussian, and multimode Brownian oscillator models. Since the models demonstrated in Figure 6 give fit results that are indistinguishable, we have arbitrarily chosen to fit the data to the one Ohmic plus two antisymmetrized Gaussians model. The resulting fits are tabulated in the Supporting Information.

Molecular Dynamics Computer Simulations of Aqueous H[−CH_2-CH($CONH_2$)−]$_7$H. The PAAm model for n=7, H[-CH_2CH(CONH_2)-]$_7$H, was simulated in a periodic box with 180 water molecules, corresponding to a concentration of 13 wt %. The MM+ all-atom force field, generalized from the MM2 parameters of Allinger,[86,87] was used as implemented in HyperChem version 5.[88] A molecular mechanics energy minimization of the isolated molecule was carried out, followed by a (gas phase) molecular dynamics run. This minimum energy helical

(61) Kinoshita, S.; Kai, Y.; Ariyoshi, T.; Shimada, Y. *Int. J. Mod. Phys. B* **1996**, *10*, 1229.
(62) Kinoshita, S.; Kai, Y.; Watanabe, Y. *Chem. Phys. Lett.* **1999**, *301*, 183.
(63) Deuel, H. P.; Cong, P.; Simon, J. D. *J. Phys. Chem.* **1994**, *98*, 12600.
(64) Cong, P.; Deuel, H.; Simon, J. D. *Chem. Phys. Lett.* **1995**, *240*, 72.
(65) Cong, P.; Simon, J. D.; She, C. Y. *J. Chem. Phys.* **1996**, *104*, 962.
(66) Wynne, K.; Galli, C.; Hochstrasser, R. M. *Chem. Phys. Lett.* **1992**, *193*, 17.
(67) Cho, M.; Du, M.; Scherer, N. F.; Fleming, G. R.; Mukamel, S. *J. Chem. Phys.* **1993**, *99*, 2410.
(68) Farrer, R. A.; Loughnane, B. J.; Fourkas, J. T. *J. Phys. Chem. A* **1997**, *101*, 4005.
(69) Loughnane, B. J.; Scodinu, A.; Farrer, R. A.; Fourkas, J. T.; Mohanty, U. *J. Chem. Phys.* **1999**, *111*, 2686.
(70) Steffen, T.; Meinders, N. A. C. M.; Duppen, K. *J. Phys. Chem. A* **1998**, *102*, 4213.
(71) Bartolini, P.; Ricci, M.; Troe, R.; Righini, R.; Santa, I. *J. Chem. Phys.* **1999**, *110*, 8653.
(72) Wang, Y.; Ushida, K.; Tominaga, Y.; Kira, A. *Chem. Phys. Lett.* **1999**, *299*, 576.
(73) Hinze, G.; Brace, D. D.; Gottke, S. D.; Fayer, M. D. *Phys. Rev. Lett.* **2000**, *84*, 2437.
(74) Hinze, G.; Brace, D. D.; Gottke, S. D.; Fayer, M. D. *J. Chem. Phys.* **2000**, *113*, 3723.
(75) Loughnane, B. J.; Fourkas, J. T. *J. Phys. Chem. B* **1998**, *102*, 10288.
(76) Loughnane, B. J.; Farrer, R. A.; Fourkas, J. T. *J. Phys. Chem. B* **1998**, *102*, 5409.
(77) Loughnane, B. J.; Farrer, R. A.; Scodinu, A.; Fourkas, J. T. *J. Chem. Phys.* **1999**, *111*, 5116.
(78) Loughnane, B. J.; Scodinu, A.; Fourkas, J. T. *J. Phys. Chem. B* **1999**, *103*, 6061.
(79) Loughnane, B. J.; Scodinu, A.; Fourkas, J. T. *Chem. Phys.* **2000**, *253*, 323.
(80) Loughnane, B. J.; Farrer, R. A.; Scodinu, A.; Reilly, T.; Fourkas, J. T. *J. Phys. Chem. B* **2000**, *104*, 5421.
(81) Fujita, H. *Polymer Solutions*; Elsevier: Amsterdam, 1990.
(82) Asaki, M. T.; Huang, C. P.; Garvey, D.; Zhou, J.; Kapteyn, H. C.; Murnane, M. M. *Opt. Lett.* **1993**, *18*, 977.
(83) Tanimura, Y.; Mukamel, S. *J. Chem. Phys.* **1993**, *99*, 9496.
(84) Palese, S.; Buontempo, J. T.; Schilling, L.; Lotshaw, W. T.; Tamimura, Y.; Mukamel, S.; Dwayne Miller, R. J. *J. Phys. Chem.* **1994**, *98*, 12466.
(85) Leggett, A. J.; Chakravarty, S.; Dorsey, A. T.; Fisher, M. P. A.; Garg, A.; Zwerger, W. *Rev. Mod. Phys.* **1987**, *59*, 1.
(86) Allinger, N. L. *J. Am. Chem. Soc.* **1977**, *99*, 8127.
(87) Berkert, U.; Allinger, N. L. *Molecular Mechanics*; American Chemical Society: Washington, DC, 1982; Vol. 177.
(88) *Hyperchem*, 5.1 ed.; Hypercube, Inc.: Gainesville, FL, 1998.

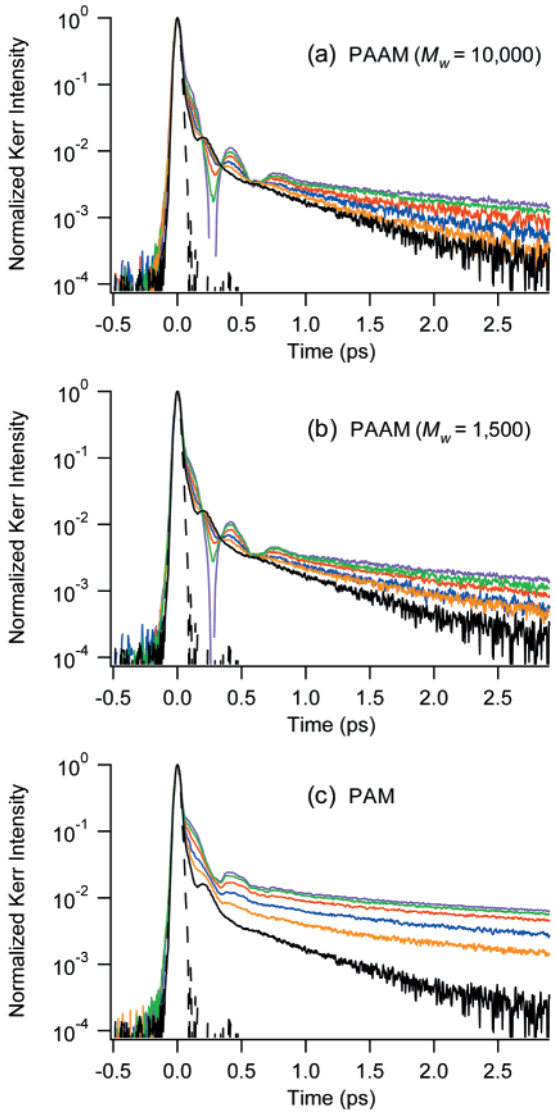

Figure 2. Short time window Kerr transients of aqueous PAAm with M_w = (a) 10 000 and (b) 1500 and (c) PrAm solutions. Purple, green, red, blue, brown, and black lines represent 40, 30, 20, 10, 5, and 0 (pure water) wt % concentration solutions, respectively. The instrument response is also shown by a black broken line.

structure was embedded in a rectangular box of volume 8,315 Å^3 together with 180 water molecules, to which periodic boundary conditions were applied. The n=7 PAAm molecule, together with the 180 water molecules in the periodic box, was first energy-minimized via molecular mechanics. This geometry provided the starting point for the molecular dynamics trajectory. This was accomplished by doing a 15 ps dynamics run where the system temperature was increased from 0 to 400 K, then run at 400 K for 10 ps, then cooled to 300 K over another 10 ps. Using these coordinates as a starting point, the dynamics trajectory that was later analyzed was run for 10 ps at 300 K. All dynamics runs were computed at 1 fs/step. Analysis of the trajectory was carried out with the gOpenMol molecular graphics program.[89]

Results

Time Domain OHD-RIKES Transients. Figure 2 shows the normalized Kerr transients for aqueous PAAm and PrAm solutions, and water, over a 3 ps time window. A strongly underdamped beat pattern occurs both in the aqueous PAAm and PrAm solutions with a shoulder near ~80 fs, and peaks near ~410 fs and ~750 fs; these underdamped dynamical features of the aqueous polymer solution increase with increasing polymer concentration. The Kerr transients of the aqueous PAAm solutions are nearly identical for both M_w = 1,500 and 10,000. For each concentration measured in this study, the Kerr transients for aqueous PAAm solutions with both molecular weights can be superposed to within the experimental noise.

Table 1. Concentrations, Shear Viscosities, and Biexponential Fit Parameters for the Diffusive Reorientational Relaxation in Aqueous PAAm and PrAm Solutions[a]

sample	concn (wt %)	X_{CRU}	η (cP)	$a_1/(a_1+a_2)$	τ_1 (ps)	$a_2/(a_1+a_2)$	τ_2 (ps)
PAAm	5	0.013	1.94	0.90	0.95	0.10	4.25
(M_w = 10 000)	10	0.027	3.64	0.88	0.90	0.12	4.88
	20	0.060	13.3	0.83	0.99	0.17	5.43
	30	0.098	53.6	0.81	1.01	0.19	6.53
	40	0.145	264	0.79	1.18	0.21	8.01
PAAm	5	0.013	1.29	0.91	0.99	0.09	4.39
(M_w = 1500)	10	0.027	1.75	0.85	0.90	0.15	5.06
	20	0.060	3.46	0.79	0.91	0.21	5.77
	30	0.098	8.61	0.79	1.02	0.21	6.76
	40	0.145	27.1	0.77	1.12	0.23	8.16
PrAm	5	0.013	1.14	0.73	0.94	0.27	5.27
	10	0.027	1.31	0.66	0.99	0.34	5.76
	20	0.058	1.72	0.64	1.11	0.36	6.88
	30	0.096	2.22	0.63	1.14	0.37	8.30
	40	0.141	2.88	0.65	1.21	0.35	9.33
water			1.00	1.00	0.93		

[a] Transients are fit from 1.0 ps time delay.

From a relative intensity analysis, we estimate that the Kerr signal arising from the polarizability anisotropy of PAAm is about 20 times that of water, similar to other aqueous amide solutions. Details of a quantum calculation (G98, MP2/6-311++G(d,p)) to estimate the gas-phase polarizability anisotropies for water and PrAm are given in the Supporting Information. The chief result is that the polarizability anisotropy for PrAm is estimated to be more than 150 times larger than that for water. The spread of electron density in the liquid resulting from hydrogen bonding should increase the relative polarizability anisotropy of water relative to that in the gas phase. Because of this, the observed polarizability anisotropy for liquid water is expected to be larger than the calculated gas-phase value.

Figure 3 shows Kerr transients of aqueous PAAm ((a) and (b)) and PrAm (c) solutions for time delays up to 36 ps. For time delays longer than 1 ps, the Kerr transients are best fit to a biexponential decay. The fits to the data are shown in Figure 3 as solid lines, with typical residuals shown above. The resulting parameters for the reorientational dynamics are listed in Table 1.

To compare concentrations for solutions of aqueous PAAm to aqueous PrAm, we define X_{CRU}, the mole fraction of the constitutional repeat unit. X_{CRU} is obtained directly from the weight percent concentration and the (partial) molecular weight of the constitutional repeat unit for the polymer solutions. For the aqueous PrAm solutions, X_{CRU} is calculated from the concentration. If the polymer is monodisperse, X_{CRU} is written as a function of the polymerization degree n and of the mole fraction of the polymer X_{PAAm} as $X_{CRU} \equiv nX_{PAAm}$.

Figure 4 plots the characteristic time constants τ_1 and τ_2 vs X_{CRU}. The fast time constant τ_1 is nearly invariant with X_{CRU}, but the slow time constant τ_2 depends strongly on the solute mole fraction X_{CRU}. The measured orientational relaxation times of aqueous PAAm solutions are the same for both 1500 and 10 000 molecular weights. The τ_2 for the PAAm solutions is slightly smaller than that for the PrAm solutions, but in both cases it is linearly dependent on the concentration X_{CRU}.

(89) Laaksonen, L. *gOpenMol*, 1.40 ed.; Center for Scientific Computing: Epsoo, Finland, 2000.

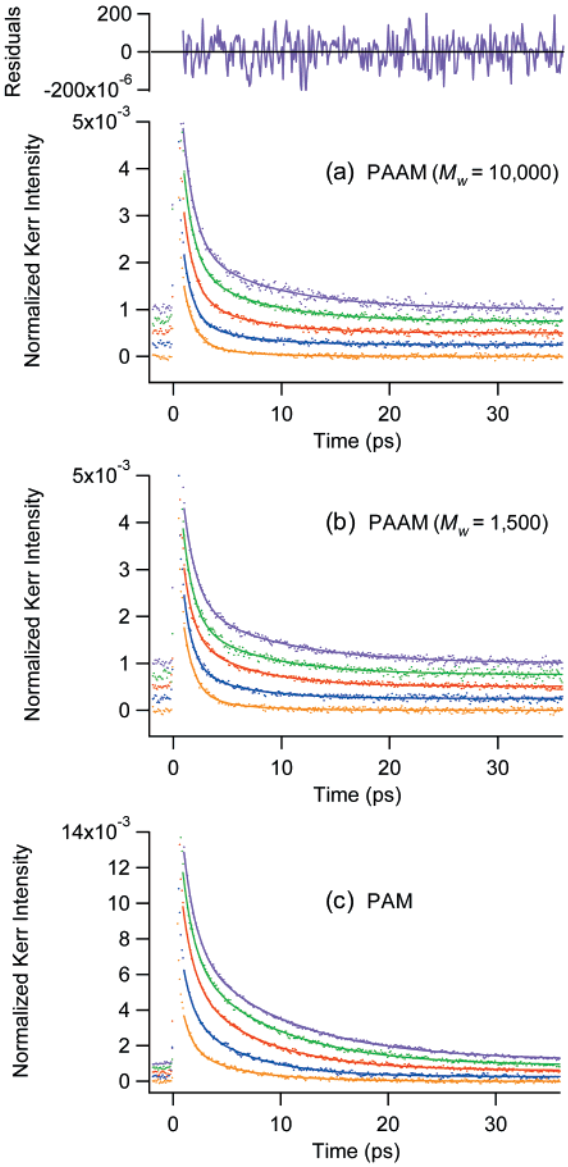

Figure 3. Longer time window Kerr transients of aqueous PAAm with M_w = (a) 10 000 and (b) 1500 and (c) PrAm solutions. Purple, green, red, blue, and brown dotted lines represent 40, 30, 20, 10, and 5 wt % concentration solutions, respectively. The biexponential fits are shown as solid lines. Residuals of the fit to the transient for aqueous PAAm with M_w = 10 000 (40 wt %) are shown at top as an example.

Frequency Domain OHD-RIKES Spectra. After Fourier transform deconvolution analysis of the OHD-RIKES transients, we obtain the spectra shown in Figure 5. Line shape analyses for the Kerr spectrum of aqueous PAAm, M_w = 10 000, are shown in Figure 6. Figure 6 demonstrates the necessity for inclusion of at least four distinct line shape functions to obtain an adequate fit to the data. The central peak at 93 cm^{-1} is assigned to the librational motions about the intermolecular hydrogen bonds, as with several other amides and aqueous amide systems.[90,91] A common interpretation for pure amide liquids is that this is an out-of-plane librational mode of a hydrogen-bonded dimer.[90,91] The high-frequency tail of the spectrum from 150 to 250 cm^{-1} is of uncertain assignment and can be fit to one or multiple line shape bands. The lowest frequency part of the intermolecular spectrum is clearly different

(90) Faurskov Nielsen, O.; Christensen, D. H.; Have Rasmussen, O. *J. Mol. Struct.* **1991**, *242*, 273.

(91) Faurskov Nielsen, O.; Lund, P.-A.; Praestgaard, E. *J. Chem. Phys.* **1982**, *77*, 3878.

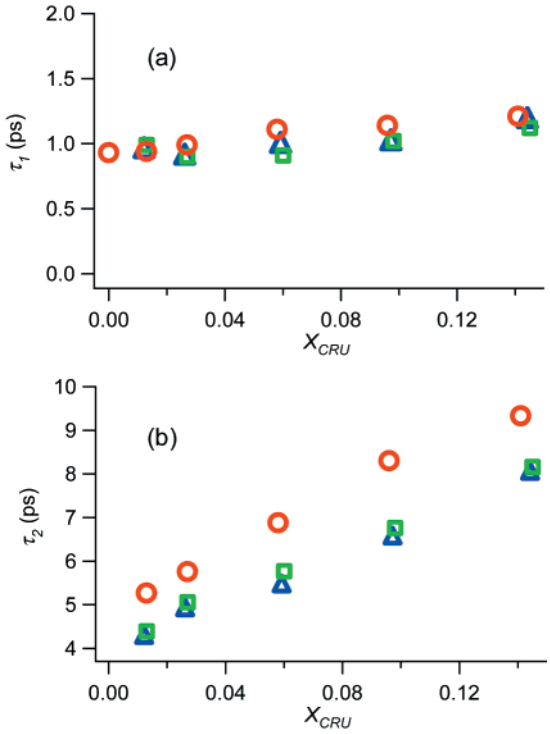

Figure 4. Dependence of the diffusive relaxation times (a) τ_1 and (b) τ_2 on the effective mole fraction of constitutional repeat unit X_{CRU} in solutions of aqueous PAAm with M_w = 10 000 (blue triangles) and 1500 (green squares) and aqueous PrAm (red circles).

for aqueous PAAm compared to that for aqueous PrAm. The line shape analyses show that the underlying spectral components for both PAAm and PrAm have the same origin but appear different because they have different relative amplitudes.

Viscosity. The shear viscosity depends strongly on both the concentration and the molecular weight. The values of the shear viscosity at 293 K for the aqueous PAAm and PrAm solutions are summarized in Table 1. For the highest concentrations studied of 40 wt %, the 264 cP viscosity value for the M_w = 10 000 PAAm solution is about 10 times larger than that of the M_w = 1500 PAAm solution (27.1 cP) and is about 100 times larger than that for aqueous PrAm (2.88 cP). In contrast to the exponential shear viscosity increase with concentration in aqueous PAAm solutions illustrated in Figure 7a,b, the shear viscosity in aqueous PrAm solutions depends linearly on X_{CRU} as shown in Figure 7c.

Molecular Dynamics Simulations of H[−CH_2CH(CO-NH_2)−]$_7$H in Water. The goal of these simulations was to make qualitative observations of both main chain and side group torsional motions. The n = 7 PAAm molecule that was simulated is shown in Figure 1a. Colored arrows highlight the torsional angles analyzed from the dynamics trajectory. Green arrows indicate the formamido side group torsions; magenta arrows indicate some of the main chain C_α−C_β torsions. The C−N bonds in the formamido side groups are much less flexible because of the partial double bond character of the amide bond.

Analysis of the MD simulations focuses on those dynamical features most likely to contribute to the Kerr depolarization—the changes in torsional angles connecting the formamido side groups to the polymer backbone, and the torsions about the main-chain (C_α−C_β) backbone (Figure 1a, yellow bonds).

For the torsions of the side groups on the third, fourth, and fifth repeat units of the n = 7 PAAm molecule, clear librational behavior is observed. The single-sided time autocorrelation

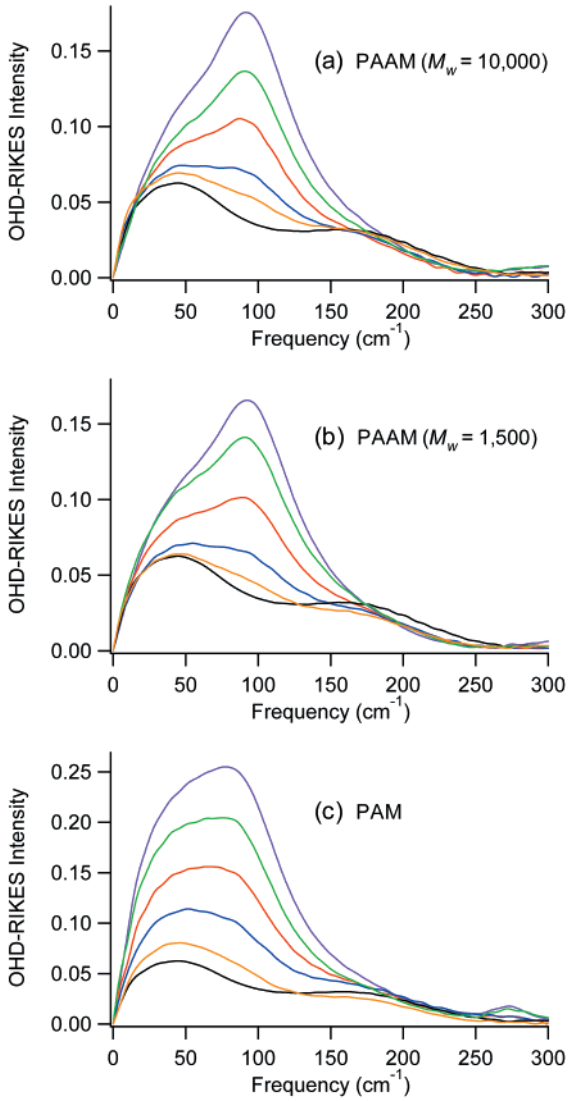

Figure 5. Low-frequency Kerr spectra of aqueous PAAm with M_w = (a) 10 000 and (b) 1500 and (c) PrAm solutions. Purple, green, red, blue, brown, and black lines represent 40, 30, 20, 10, 5, and 0 (pure water) wt % concentration solutions, respectively.

functions for the bond torsional dynamics show maxima at 20, 50−60, 100, and 200−250 fs. These time constants are reminiscent of those observed in both water[32,33] and formamide[43] Kerr dynamics. The root-mean-square fluctuations for side group torsions on the third, fourth, and fifth repeat units average to 20°. Large angle changes in conformation are not observed for the side groups of these three CRUs. Librations also are observed for the main chain torsions of these three CRUs. A large angle jump of about 90° occurs after 4 ps for a main chain torsion of the fifth repeat unit. Hydrocarbon torsions along the main chain show 11° RMS fluctuations of torsion angles.

Discussion

PAAm Reorientational Dynamics: Dependence of the Time Constants on Concentration and Chain Length. Reorientational dynamics in polymer solutions are substantially more complex than those for either neat solvents or solutions of low-molecular-weight rigid molecular solutes. For dilute polymer solutions, spectroscopically measured reorientation dynamics may include several contributions. From slowest to most rapid, these motions include rotation of the overall polymer chain, collective twisting of segments (consisting of several CRUs), reorientation of (and within) individual CRUs, and librations between the main chain and side groups within a single CRU. Both semidilute and concentrated polymer solutions have the further complexity of interactions and entanglements between polymer chains. Aqueous polymer dynamics may be even more complicated because of strong hydrogen-bonding interactions that occur between water and polymer, and from polymer to polymer. In some cases, water may bridge polymer segments via multiple hydrogen bonds. Concentrations used in our experiments on aqueous PAAm encompass all of the above paradigms.

For a wide range of solutions, the diffusive orientational dynamics of both solvent and solute have been found to obey Stokes−Einstein−Debye hydrodynamic scaling laws. The Stokes−Einstein−Debye (hydrodynamic) model for the rotational dynamics of a spherical particle in simple solutions predicts that the reorientation time constant is $\tau_s = 3V\eta/k_BT$, where V is the volume of the particle, η is the viscosity of the medium, k_B is the Boltzmann constant, and T is the absolute temperature.[92] Common experimental methods for measuring these dynamics are time-resolved absorption or fluorescence polarization spectroscopies and nonlinear optical methods including OHD-RIKES. As we discuss below, the longest time scale diffusive reorientation dynamics (observed by OHD-RIKES) for the aqueous PrAm solutions show a linear dependence of reorientation lifetime on viscosity.

In complex polymer environments, the simple hydrodynamic description of diffusive reorientation dynamics breaks down. One example of this behavior is the depolarized Rayleigh work on polystyrene solutions by Bauer et al.[93] They showed that two relaxation modes exist in polystyrene solutions with $M_w > 10^4$. On increasing the molecular weight from $M_w = 10^4$ to 2×10^6, the longer relaxation time constant increased from 10 ns to 73 μs. The second, faster relaxation time varied from 3.2 to 5.7 ns for the same range of M_w and was assigned to segmental dynamics. Sengupta, Terazima, and Fayer studied the dynamics of poly(2-vinylnaphthalene) in CCl_4 solution by the transient-grating optical Kerr effect (TG-OKE) method using a subpicosecond laser. Over a wide range of temperatures and viscosities, they found that the observed dynamics were best assigned to motions of the naphthalene side groups, and a complete breakdown of simple hydrodynamic theory was found.[94] Sengupta and Fayer gave another example of nonhydrodynamic orientational relaxation in their work on poly(methylphenylsiloxane) (PMPS), both in the melt and in CCl_4 solution.[95] In the melts of the glass-forming PMPS, triexponential orientational dynamics (with lifetimes of about 2.3, 11.5, and 105 ps) were shown to be invariant with temperature, showing no change for values of η/T that spanned a range greater than a factor of 40. Similar (but not identical) results were obtained for PMPS solutions in CCl_4. Assignment of the reorientation dynamics to the phenyl side group was made by comparison of PMPS to poly(dimethylsiloxane), for which the TG-OKE signal was reduced in intensity by a factor of 400, and no orientational dynamics longer than 1 ns were observed. For the TG-OKE studies on PMPS melts, hydrodynamic theories for the reorientational dynamics do not apply; instead, power law decays are observed.[95] Though we varied the viscosity of aqueous PAAm and PrAm solutions by changing concentration,

(92) Fleming, G. R. *Chemical Applications of Ultrafast Spectroscopy*; Oxford University Press: New York, 1986.
(93) Bauer, D. R.; Brauman, J. I.; Pecora, R. *Macromolecules* **1975**, *8*, 443.
(94) Sengupta, A.; Terazima, M.; Fayer, M. D. *J. Phys. Chem.* **1992**, *96*, 8619.
(95) Sengupta, A.; Fayer, M. D. *J. Chem. Phys.* **1994**, *100*, 1673.

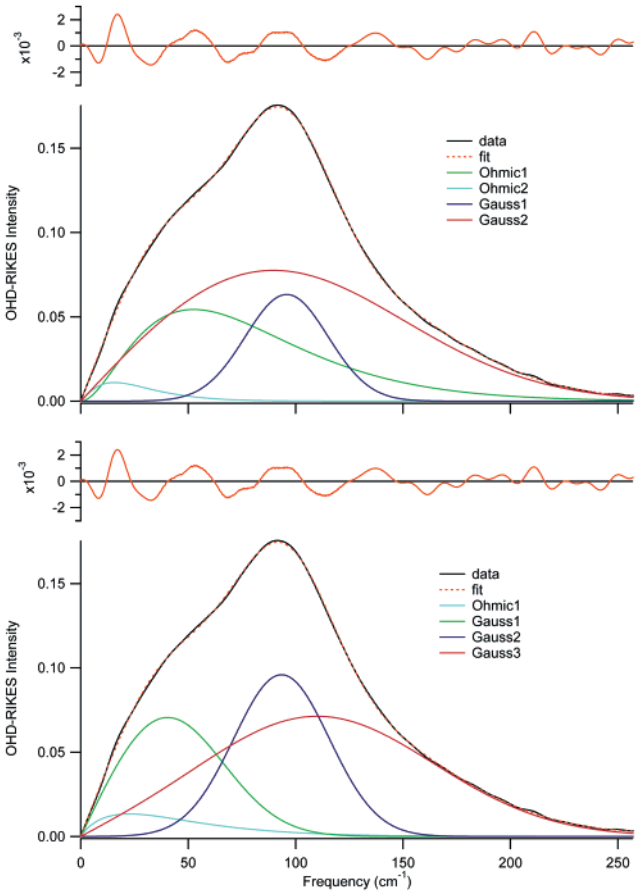

Figure 6. Line shape analyses of low-frequency OHD-RIKES spectra for 40 wt % aqueous PAAm, $M_w = 10\,000$. Top: Fitted line shape is a sum of two Ohmic and two antisymmetrized Gaussian functions. Bottom: Line shape is a sum of one Ohmic and three antisymmetrized Gaussian functions. Tabulated results are available in the Supporting Information. Note that while the component line shapes differ substantially, the quality of fit, evidenced by the fit residuals, is identical.

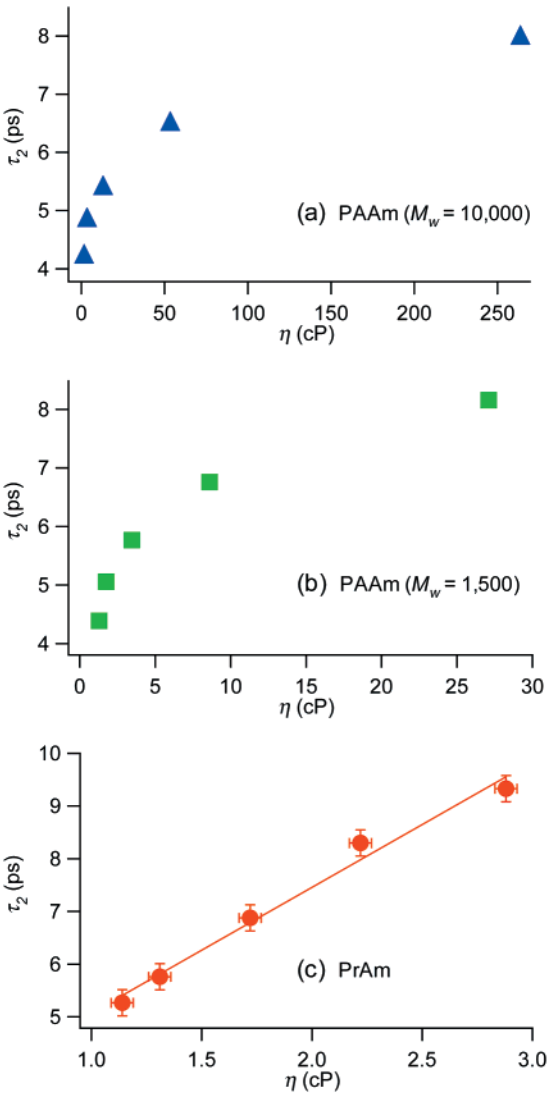

Figure 7. Shear viscosity η dependence of the slower reorientational time constant τ_2 for aqueous PAAm with (a) $M_w = 10\,000$ and (b) 1500 and (c) PrAm solutions.

not temperature, our results also disagree with simple hydrodynamic models, vide infra. Matsuo et al. observed ^{19}F NMR T_1 relaxation dynamics of labeled polystyrenes in various solvents. The observed dynamics were also independent of polymer molecular weight for $M_w > 10^4$.[96] Last, Mashimo et al. observed dielectric relaxation phenomena for dilute poly(propylene oxide) solutions in benzene with a clear separation of dynamics into two bands: a fast motion of ~70 ps that is independent of M_w, and a slower ~1 ns motion that increases linearly with log M_w.[97]

A number of other works have also shown that the trimodal description of polymer reorientation dynamics applies to both solution and melt samples. Methods used include NMR, dielectric relaxation, and computer simulations.[98] In agreement with the Fayer group's work,[95] Ediger and co-workers have consistently assigned polymer melt dynamics to librational, segmental, and entire polymer orientational motions for both polyethylene[99] and polypropylene.[100] Molecular dynamics simulations on polyisoprene melts also support this concept.[101] Kaatze et al. also observed three dielectric relaxation times for aqueous poly(vinyl alcohol) and poly(ethylene oxide) solutions. They assigned the three observed dielectric relaxation modes to bulk water, reorientation of bound waters of hydration, and segmental motions of the polymer.[102]

For the OHD-RIKES transients of the aqueous PAAm and PrAm solutions, a biexponential model for the reorientation dynamics is required. This is in agreement with almost all prior Kerr measurements, including those on liquid water.[31−35,84] Liquid water has at least a biexponential response but fits reasonably to an averaged single-exponential decay of about 1.0 ps. Table 1 shows that the faster reorientation time constant τ_1 is only very weakly dependent on the concentration X_{CRU}. We have studied several other aqueous solutions, including 1-propanol, urea, guanidinium, DMSO, and three formamides, and the same result obtains: over the entire range of concentration, a faster 1 ps orientational relaxation is found with a value of about $\tau_1 = 1 \pm 0.1$ ps. (*Note that the 1.0 ps result depends on the delay time at which the fit begins; in this work, all fits were started at 1.0 ps.*) A simple reason to assign this value of $\tau_1 = 1$ ps to water reorientation is that none of the other liquids

(96) Matsuo, K.; Kuhlmann, K. F.; Yang, H. W.-H.; Geny, F.; Stockmayer, W. H. *J. Polym. Sci.: Polym. Phys. Ed.* **1977**, *15*, 1347.
(97) Mashimo, S.; Yagihara, S.; Chiba, A. *Macromolecules* **1984**, *17*, 630.
(98) Ediger, M. D.; Adolf, D. B. *Adv. Polym. Sci.* **1994**, *116*, 73.
(99) Qiu, X.-H.; Ediger, M. D. *Macromolecules* **2000**, *33*, 490.
(100) Qiu, X.-H.; Moe, N. E.; Ediger, M. D. *J. Chem. Phys.* **2000**, *113*, 2918.
(101) Moe, N. E.; Ediger, M. D. *Polymer* **1996**, *37*, 1787.
(102) Kaatze, U.; Gottmann, O.; Podbielski, R.; Pottel, R.; Terveer, U. *J. Phys. Chem.* **1978**, *82*, 112.

or solutes are small enough to reorient this quickly. Another piece of supporting evidence is the work of Cabral et al. on 2:1 mixtures of aqueous DMSO using quasi-elastic neutron scattering. They studied this composition of aqueous DMSO over the temperature range from 246 to 300 K. For each temperature, they obtained a water diffusive reorientation time constant of 1.0 ps, clearly indicating that Stokes−Einstein−Debye hydrodynamics cannot apply for the water reorientation in aqueous DMSO.[103] Together with our work on the eight aqueous solutions, which show only a weak concentration dependence of short lifetime τ_1, the result reported by Cabral et al. on water reorientation in the 2:1 H_2O/DMSO solutions provides circumstantial evidence that water may have a more universal reorientation time of about 1 ps under many conditions.

Molecular reorientation time constants scale with viscosity, temperature, and molecular volume in hydrodynamic theories, as well as in certain limits for polymer dynamics. In the present experiments, the temperature is held constant so that the relevant variables for the reorientational dynamics are the viscosity and the solute volume. The measured bulk viscosity dependence for τ_2 of the PAAm and PrAm solutions is shown in Figure 7. The partial volume of the constitutional repeat unit $V(-CH_2CH(CONH_2)-)$ estimated from van der Waals increments is 65 Å^3. The molecular volume of PrAm is 77 Å^3.

First, we consider the rotational motion of the entire polymer, compared with estimates of molecular volumes. Orientational motions of the entire macromolecule are often described by the autocorrelation of a vector between the first and the last constitutional repeat units.[13−16] NMR measurements of both solutions and melts show reorientation time constants in the nanosecond and microsecond range (depending on the molecular weight).[98] In the transient grating optical Kerr effect experiments on poly(2-vinylnaphthalene) in CCl_4, Fayer and co-workers reported that there was no relaxation observed with a time constant longer than 105 ps.[94] However, the relative amplitudes of the reorientational motions for the entire polymer chain are less than 2% of that for either the diffusive or librational side group reorientations.[99,100]

For concentrated polymer solutions, the rotational diffusion time, τ_r, of the entire polymer chain in solution depends strongly on the polymerization degree, n: $\tau_r \propto \langle n \rangle^x$.[15,16] Data for a number of (nonaqueous) polymer solutions show that both τ_r and viscosity scale as $n^{3.4}$. However, the slowest reorientational time constants τ_2 for aqueous PAAm solutions are independent of molecular weight. Thus, the slowest time constants of 4−10 ps in aqueous PAAm solutions that we observed in this study cannot be assigned to the reorientational relaxation process of the entire polymer.

Consider the reorientational motions of the PAAm side groups. The partial volume of the formamido side group ($-CONH_2$, V_{CONH_2}) estimated from van der Waals increments is 37 Å^3. The ratio of the volumes for the PAAm side group to PrAm is $V_{CONH_2}/V_{PrAm} = 0.48$. However, the average ratio of the slower reorientation time constants of aqueous PAAm and PrAm solutions, τ_2(PAAm)/τ_2(PrAm), is 0.83 for samples at all aqueous solution concentrations measured in this study. Fayer and co-workers suggested that the picosecond dynamics of poly(2-vinylnaphthalene) in CCl_4 arise from the orientational relaxation of the naphthalene moiety since the main chain remains rigid on the time scale of the picosecond naphthalene reorientation.[94] For longer chain polymers, several groups reported either null or negligible dependence of local polymer motions on the polymerization degree.[98,104−106]

(103) Cabral, J. T.; Luzar, A.; Teixeira, J.; Bellissent-Funel, M.-C. *J. Chem. Phys.* **2000**, *113*, 8736.

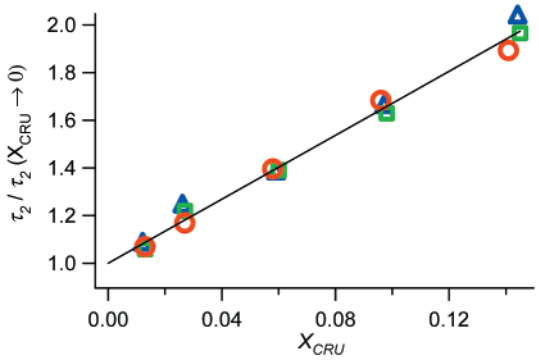

Figure 8. Plots of the normalized slower diffusive relaxation times $\tau_2/\tau_2(X_{CRU} \rightarrow 0)$ of aqueous PAAm (with $M_w = 10\,000$ (blue triangles) and 1500 (green squares) and PrAm (red circles) solutions) vs the effective mole fraction of the constitutional repeat unit X_{CRU}.

PAAm is a flexible polymer, so we next consider the dynamics of the individual constitutional repeat units. The ratio of the volume for the PAAm CRU to that of PrAm is 65/77 = 0.845. As shown in Figure 4 and Table 1, at a given concentration these volume ratios equal the ratio of the observed time constants for reorientation, τ_2(PAAm)/τ_2(PrAm). The reorientation time constant for the PAAm CRU is 83% of that of PrAm. This implies that the local friction experienced by a single unit $-CH_2CH(CONH_2)-$ is very similar to that experienced by PrAm ($CH_3CH_2CONH_2$). This should not be surprising, since for a given concentration X_{CRU}, the same kinds of dipole−dipole interactions and hydrogen bonds occur. Because PAAm is moderately flexible, torsional motions of the formamido side groups and between adjacent $-CH_2CHCONH_2-$ repeat units will depolarize the Kerr transient on a time scale much faster than rotational motions of the entire polymer chain.

A graphical representation of the equivalence of reorientational friction between the aqueous PAAm and PrAm is given in Figure 8. By plotting the longer reorientation time constant τ_2 (normalized by its intercept at infinite dilution) vs the mole fraction X_{CRU}, one finds that the data for both molecular weights of PAAm and for PrAm are all linear and are all superposable to within error.

There are both similarities and differences between our observed dynamics in aqueous polyacrylamide solutions and the previous work in the literature on poly(2-vinylnaphthalene)[94] and PMPS[95] solutions, and melts of polyethylene[99] and polypropylene.[100] The local environment of the aqueous PAAm is wholly different in character relative to the other hydrophobic polymers because of its strongly interacting, hydrogen-bonding solute−solvent interactions. However, the concept developed for the nonpolar polymers, that the polymer dynamics probed on a local scale involve side groups (for bulky substituents such as phenyl and naphthyl groups) or entire repeat units, is qualitatively the same picture obtained from analysis of our Kerr transients in the diffusive relaxation time regime.

Ultrafast Dynamics: Underdamped Intermolecular Vibrations in Aqueous PAAm Solution. Comparison of the concentration dependence of the low-frequency Kerr spectra for aqueous PAAm and PrAm solutions (Figure 5) shows the following. The amplitude of the 93 cm^{-1} band becomes larger with increasing concentration for both the PAAm and PrAm aqueous solutions. The contribution of the lowest-frequency

(104) Heatley, F. *Annu. Rep. NMR Spectrosc.* **1986**, *17*, 179.
(105) Fixman, M. *J. Chem. Phys.* **1978**, *69*, 1538.
(106) Zuniga, I.; Bahar, I.; Dodge, R.; Mattice, W. L. *J. Chem. Phys.* **1991**, *95*, 5348.

band ($\sim$40 cm^{-1}) in the aqueous PAAm solution is smaller than that in the aqueous PrAm solution. The Kerr spectra for aqueous PAAm are superposable for both molecular weights. The aqueous PAAm spectra display more pronounced underdamped transients than have been observed previously for any other liquids or solutions; the Kerr transient oscillations even cross into negative territory for the 40 wt % solutions. The apparent cause is a relative shift in amplitudes between the central band that peaked at 93 cm^{-1} and the broad, lower frequency band at 40 cm^{-1}. The aqueous PAAm Kerr spectra show a diminished amplitude of the 40 cm^{-1} band compared to the Kerr spectra of aqueous PrAm, formamide, *N*-methylformamide, or *N*,*N*-dimethylformamide.

By analogy with the Kerr spectra for other amides, a librational band in the 40−60 cm^{-1} range is to be expected, because of the large dipole moment of the formamido side group of about 4 D.[42,43,46] By analogy with numerous studies using Kerr, low-frequency Raman, far-IR spectroscopy, and molecular dynamics and instantaneous normal mode simulations, we assign the 90 cm^{-1} band in the aqueous PAAm and PrAm solutions to librational dynamics about N−H···O hydrogen bonds.[42,43,46,90,91,107−110] With the amide N−H donor, it is possible to form two different types of hydrogen bonds: N−H···O═C (to another formamido side group) and N−H···OH$_2$ (to water). Hydrogen bonds from water donation to amide carbonyls may also be contributing to the Kerr spectral density in aqueous PAAm and PrAm solutions. Kerr spectra of aqueous PAAm solutions resemble the spectra of both aqueous formamide and PrAm solutions for mole fractions $X_{CRU} = 0.10$, 0.15.[111]

Conclusions

Using femtosecond optical heterodyne-detected Raman-induced Kerr effect spectroscopy, we have investigated the ultrafast dynamics for aqueous solutions of polyacrylamide (PAAm) and the model for the PAAm constitutional repeat unit, propionamide (PrAm). The reorientational dynamics for aqueous PAAm solutions, with time constants τ_2 ranging from 4 to 9 ps, are not correlated with the macroscopic shear viscosity. However, this reorientation time constant is well correlated with the mole fraction of constitutional repeat units X_{CRU} for the aqueous solutions of both molecular weights of PAAm, and also for aqueous PrAm solutions. This indicates that the dynamics of aqueous PAAm affecting the molecular polarizability anisotropy must occur predominantly on the length scale of individual CRUs. Our simple molecular dynamics calculations fully support this picture. The reorientation time constants (normalized by the intrinsic reorientation time constants at infinite dilution) are linearly proportional to concentration for both the PAAm and PrAm aqueous solutions, with identical slopes for each of the three samples (to within error). The intermolecular interactions between aqueous PAAm and PrAm solutions are very similar, in terms of both hydrogen bonds and dipolar interactions. Thus, it is reasonable to assume that the local friction for reorientation of a single CRU of the PAAm may be similar to that experienced by PrAm, since no correlation between polymer reorientation time constants and macroscopic shear viscosity is observed.

Dynamics in the femtosecond time regime for aqueous PAAm solutions cause more strongly underdamped transients to be observed relative to aqueous PrAm solutions. From the Fourier transform analysis of the time-domain Kerr data, it becomes clear that the strongly underdamped dynamics in the PAAm solution arise from a reduction in relative intensity of the intermolecular band near 40 cm^{-1} in the PAAm solutions versus the PrAm solutions.

Acknowledgment. We thank Prof. Kazuyuki Horie (University of Tokyo) and Prof. Mark Ediger (University of Wisconsin) for suggestions and fruitful discussions. We also thank Mr. Jonathan Harris and Dr. Piotr Wiewiór (both of Rutgers University) for their assistance during the initial setup of the lab-built Ti:sapphire laser and Kerr experiment.

Supporting Information Available: Details of experimental methods and OHD-RIKES data analysis and evaluation of the polarization anisotropy for PrAm and water from MP2 calculations (PDF). This material is available free of charge via the Internet at http://pubs.acs.org.

JA010290Z

(107) Itoh, K.; Shimanouchi, T. *Biopolymers* **1967**, *5*, 921.
(108) Itoh, K.; Shimanouchi, T. *J. Mol. Spectrosc.* **1972**, *42*, 86.
(109) Goossens, K.; Smeller, L.; Heremans, K. *J. Chem. Phys.* **1993**, *99*, 5736.
(110) Torii, H.; Tasumi, M. *J. Phys. Chem. A* **2000**, *104*, 4174.
(111) Wiewior, P. P.; Shirota, H.; Castner, E. W., Jr., unpublished.